Hindawi
Mathematical Problems in Engineering
Volume 2017, Article ID 2095896, 6 pages
https://doi.org/10.1155/2017/2095896

Research Article

A Method for Identification of Transformer Inrush Current Based on Box Dimension

Maofa Gong,[1] Ran Zheng,[1] Linyuan Hou,[1,2] Jingyu Wei,[1] and Na Wu[1]

[1]*College of Electrical Engineering and Automation, Shandong University of Science and Technology, Qingdao, Shandong 266590, China*
[2]*State Grid Shandong Electric Power Maintenance Company, Jinan, Shandong 250021, China*

Correspondence should be addressed to Ran Zheng; 137626604@qq.com

Received 10 July 2017; Accepted 23 October 2017; Published 19 November 2017

Academic Editor: Anna M. Gil-Lafuente

Magnetizing inrush current can lead to the maloperation of transformer differential protection. To overcome such an issue, a method is proposed to distinguish inrush current from inner fault current based on box dimension. According to the fundamental difference in waveform between the two, the algorithm can extract the three-phase current and calculate its box dimensions. If the box dimension value is smaller than the setting value, it is the inrush current; otherwise, it is inner fault current. Using PSACD and MATLAB, the simulation has been performed to prove the efficiency reliability of the presented algorithm in distinguishing inrush current and fault current.

1. Introduction

Longitudinal differential protection, as a part of main protection, can identify the inner fault and outer fault effectively in transformer. When an external fault of transformer is cleared or a no-load transformer is input, the high amplitude of inrush current will be generated [1], which can lead to maloperation of differential protection. In recent years, the accelerated construction of global energy interconnection, the increased capacity of transformers, and improved level of voltage have put forward higher requirements for transformer protection. Therefore, the accurate identification of inrush current is particularly critical [2].

Nowadays, there are three algorithms that are widely used in identification of inrush current: second harmonic discriminance, dead angle discriminance, and waveform symmetry discriminance. Due to the increase of the transformer capacity and the change of the core material, the second harmonic content in the inrush current will reduce. And long transmission line inductance and distributed capacitance may increase the second harmonic content. So, the change of second harmonic in power system reduces the accuracy of the second harmonic discriminance. The dead angle discriminance and the waveform symmetry discriminance have high requirements on the sampling frequency and are subject to the saturation of the current transformer. In view of shortages of above algorithms, many scholars have proposed improved algorithms or new algorithms. In literature [3], after the wavelet transform of signal, modular maximum can be extracted to identify inrush current. Although the algorithm has a high accuracy, the wavelet transform is of heavy computation and difficult when selecting basis function. Literature [4] proposed that Hilbert marginal spectrum can identify the inrush current, but there is a problem of oversampling. Literature [5] proposed grid fractal to obtain the changing curve of grid. The frequency characteristic of the changing curve can identify the inrush current, but the algorithm is short of fast motion. In literature [6], the proposed algorithm of combining wavelet transform with neural network has a high accuracy. However the neural network needs a lot of samples to train classifier. Literature [7] proposed that the morphological gradient of the sampled signal can be extracted by mathematical morphology. And its waveform area can be used to identify the inrush current.

Fractal is proposed by Mandelbrot in 1982. Fractal is widely used in complex and irregular graphics description [8]. And it can process digital signal simply and quickly. Fractal also can quantify unordered behavior and does not require the same pace between signal frequency and sampling frequency and does not need time-frequency transformation.

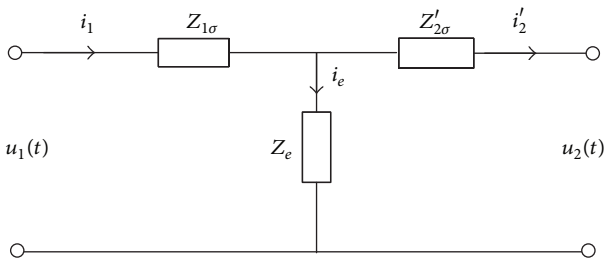

Figure 1: Transformer equivalent circuit after converting to primary side.

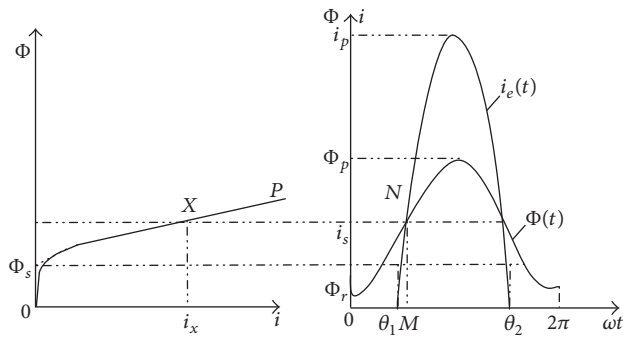

Figure 2: Generating mechanism of inrush current.

So, it is suitable for real-time signal processing [9]. In this paper, the box dimension of fractal is applied to the identification of inrush current.

2. Theoretical Analysis of Inrush Current

In this paper, the single-phase transformer is used to analyze the producing mechanism of the inrush current. Its equivalent circuit is shown in Figure 1.

Denote winding voltage as $u_1(t) = U_m \sin(\omega t + \alpha)$ in steady-state operation. According to Faraday's law of induction, as transformer is no-load and closing, using differential equation of $u_1(t) = d\Phi/dt$, the core flux Φ can be calculated as

$$\Phi = \int u_1(t)\, dt = -\Phi_m \cos(\omega t + \alpha) + C, \tag{1}$$

where $\omega = 100\pi$ and $\Phi_m = U_m/\omega$. C is integral constant, and its value is connected with voltage and magnetic flux in no-load closing time ($t = 0$). Let the core remnant be Φ_r; then

$$C = \Phi_m \cos\alpha + \Phi_r. \tag{2}$$

When the no-load transformer is closed, the magnetic flux in the transformer core is

$$\Phi = -\Phi_m \cos(\omega t + \alpha) + \Phi_m \cos\alpha + \Phi_r, \tag{3}$$

where $\Phi = -\Phi_m \cos(\omega t + \alpha)$ is steady-state flux. It is a periodic sinusoidal quantity. $\Phi_m \cos\alpha + \Phi_r$ is a transient flux. Considering the transformer loss, it is a aperiodic component and decays with time. If $\Phi_m \cos\alpha$ is in phase with Φ_r, then the core flux reaches the maximum $\Phi_p = 2\Phi_m \cos\alpha + \Phi_r$ at $t = \pi$. Obviously, the maximum flux generated during no-load closing may be much larger than the saturated flux Φ_s of the transformer, which makes the iron core saturation.

In Figure 2, when $\Phi < \Phi_s$, the core does not reach saturation, so the impedance of magnetizing branch is large. And the excitation current i_e is far less than i_s. In this case, i_e can be neglected. When $\Phi > \Phi_s$, the core enters into the saturated state. Then the impedance of excitation branch decreases. The excitation current increases sharply and forms magnetizing inrush current where amplitude i_p may be up to 6–8 times the rated current.

Based on the above theoretical analysis, the magnitude of inrush current is related to the initial phase angle α of voltage when closing breaker, the voltage amplitude U_m, the saturation flux Φ_s, and the size and direction of the remanence Φ_r in the core. In addition, inrush current of three-phase transformer is also related to its wiring methods [10].

3. Introduction of Box Dimension Algorithm

The basic property of fractal is the local self-similarity of the signal at different scales. The signal of inrush current is a nonstationary signal with singularity. And the singular signal has statistical self-similarity. This kind of self-similarity provides the basis for fractal analysis.

The singularity of the signal is usually described by the Lipschitz (Lip) exponent a. For the function $f(t)$, and $0 \le a \le 1$, given constant A and $h_0 > 0$, when $0 < h < h_0$, if

$$\left| f(t_0 + h) - f(t_0) \right| \le Ah^a \tag{4}$$

then function $f(t)$ has the Lip exponent a at t_0. If a is a positive number, assume $n \le a < n + 1$, n is an integer, the function $f(t)$ will be differentiable of n order at t_0, and the nth derivative is point singularity at t_0. If $a = 1$, the function $f(t)$ also will be differentiable at t_0, and the derivative is bounded and discontinuous. If $0 < a < 1$, the function $f(t)$ will be singularity at t_0. If $a = 0$, the function $f(t)$ is discontinuous and bounded at t_0. If $a < 0$, the function $f(t)$ is singularity at t_0.

Lip exponent can reflect the degree of signal similarity. The greater the value of a, the higher the degree of similarity about the self-similar process. Self-similar process has fractal features. Its fractal dimension D is associated with Lip index a. There are many algorithms to calculate the fractal dimension, and the calculation and experience estimation of box dimension are simpler than other algorithms.

This paper defines a simplified method for calculating the box dimension D of a one-dimensional discrete signal. Before calculating the box dimension in the plan set F, we can first make a δ coordinate grid intersecting set F on the plane, as shown in Figure 3 [11].

For a discrete digital signal, the size of the square grid δ is chosen as the reciprocal of sampling frequency f.

The formula of $N_\delta(F)$ is as follows:

$$N_\delta(F) = \frac{1}{\delta} \sum_{i=1}^{n} \left| x_i - x_{i+1} \right|, \tag{5}$$

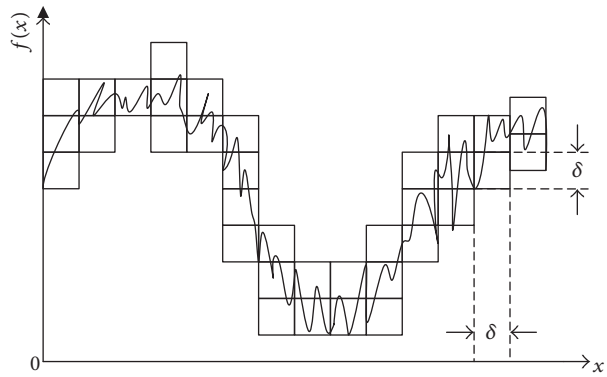

Figure 3: Definition of box number.

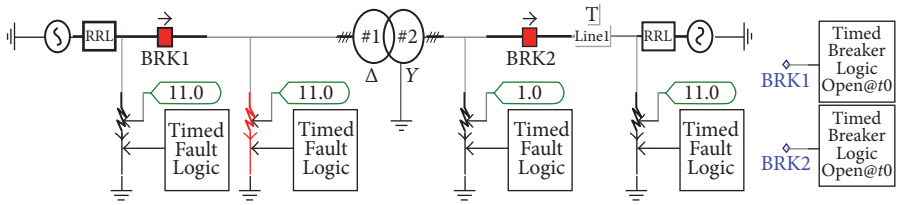

Figure 4: Simulation model of three-phase transformer inrush current.

where x_i, x_{i+1} are the sampling points and n is the number of sampling points in a cycle and is even.

The grid size is increased to 2δ; the number $N_{2\delta}(F)$ intersecting grids can be calculated as follows:

$$N_{2\delta}(F) = \frac{1}{2\delta}\sum_{i=1}^{n/2}\left(\max\left(x_{2i-1}, x_{2i}, x_{2i+1}\right) - \min\left(x_{2i-1}, x_{2i}, x_{2i+1}\right)\right). \quad (6)$$

The box dimension D is defined as follows:

$$D = \frac{\lg\left(N_{\delta}(F)\right) - \lg\left(N_{2\delta}(F)\right)}{\lg\delta^{-1} - \lg(2\delta)^{-1}}. \quad (7)$$

Each sampled signal has a unique value about box dimension D. The values about different signals are generally not the same. Thus, the box dimension D can be used as an eigenvalue for signal identification.

4. Simulation Study on Inrush Current and Inner Fault Current

Through the PSCAD, the model of inrush current about three-phase transformer [12] was established as shown in Figure 4.

The transformer of SFPZ7-120000/220 is selected as power transformer in simulation. Its wiring way is YNd11 and variable ratio is 220/35 kV. Modules (BRK1 and BRK2) of circuit breaker are used to control the breaking of circuit [13]. And the different transformer parameters are set to simulate the inrush current in different circumstances. At the beginning of the simulation, the circuit breakers are disconnected. And the circuit breaker BRK1 is closed at 0.1 s. The current waveform of A phase is shown in Figure 5.

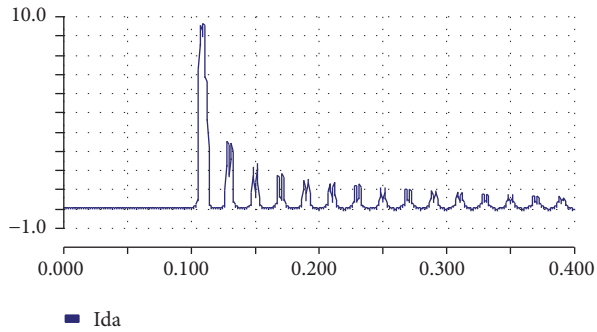

Figure 5: Waveform of inrush current.

From Figure 5, we can see that the inrush current waveform has serious distortion. Its amplitude is large and dead angle exists.

Through setting four fault modules on both sides of transformer, different types of inner fault and outer fault in Δ side and Y can be simulated. The inner faults of transformer differential protection (including interturn short circuit, ground fault, and phase short circuit) can be divided into the inner faults in normal operation and the inner faults in transformer no-load closing. Then the simulation results of the above two cases are analyzed to identify the difference of differential currents.

At 0.1 s, the Δ side in normal operation is set to have three-phase ground fault. Differential current of A phase is shown in Figure 6.

A phase differential current, when the Δ side in no-load closing has the three-phase ground fault, is shown in Figure 7.

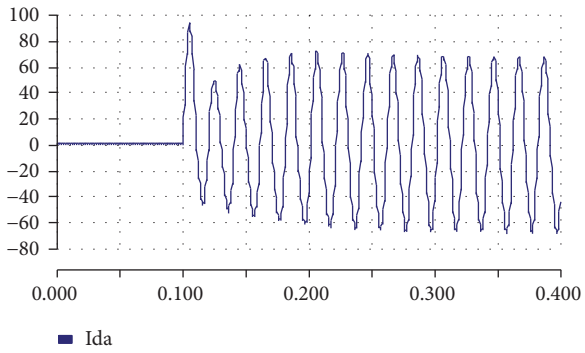

Figure 6: Waveform of inner fault current (fault occurs in normal operation).

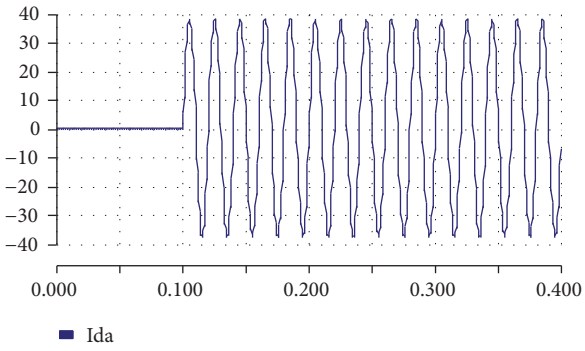

Figure 7: Waveform of transformer inner fault current (fault occurs in no-load closing).

The simulation model shown in Figure 4 cannot simulate interturn fault of three-phase transformer. Thus, we use three single-phase three-winding transformers to form a three-phase transformer. The secondary windings of two transformers are connected together as a new secondary winding [14]. The fault point is set in the wiring of secondary winding. So changing the parameters of resistance and inductance in secondary winding can simulate turn-to-turn faults in different positions. The simulation model is shown in Figure 8.

The three-phase differential current in the 10% of turn-to-turn fault is shown in Figure 9.

According to the simulation results of the inner fault in Figures 6, 7, and 9, it is found that the amplitude of the differential current increases. But the waveform is basically maintained as sine wave and the amplitude of that does not decay after the fault occurs.

Compared with simulation results of Figures 5, 6, 7, and 9, the waveforms of inrush current and the inner fault current all have large amplitude. However there is a big difference in the waveforms shape. The difference in waveforms can be detected by their box dimension D which is a basis for identifying the inrush current [15].

Table 1: Box dimensions of inner fault current (faults occur in normal operation).

Fault type	D_A	D_B	D_C
Single-phase ground	1.4178	1.3780	1.4177
Two-phase short circuit	1.4174	1.4174	1.4174
Two-phase ground	1.3839	1.4174	1.3929
Three-phase short circuit	1.3804	1.4174	1.3863
Three-phase ground	1.3844	1.4174	1.3903
Turn-to-turn fault (10%)	1.4063	1.4176	1.4153
Turn-to-turn fault (20%)	1.3822	1.3955	1.4088
Turn-to-turn fault (50%)	1.3799	1.3895	1.4131

Table 2: Box dimensions of inner fault current (faults occur in no-load closing).

Fault type	D_A	D_B	D_C
Single-phase ground	1.3895	1.3913	1.3603
Two-phase short circuit	1.4117	1.4116	1.4063
Two-phase ground	1.3812	1.4116	1.3768
Three-phase short circuit	1.3839	1.4116	1.3755
Three-phase ground	1.3840	1.4116	1.3755
Turn-to-turn fault (10%)	1.3918	1.4079	1.411
Turn-to-turn fault (20%)	1.3757	1.3948	1.4087
Turn-to-turn fault (50%)	1.3844	1.3895	1.4153

5. Identification Criterion of Inrush Current Based on the Box Dimension

It is analyzed that the box dimension D can be used as the eigenvalue to distinguish the inrush current from the inner fault current. Box dimension D can be calculated according to (7). And it is compared with setting value D_{ZD} to determine whether the sampling signal is inrush current or inner fault current. The identification of the inrush current is

$$D \le D_{ZD}. \tag{8}$$

According to the various operations of the transformer, $D_{ZD} = 1.38$ is determined ultimately.

D_A, D_B, D_C are box dimension of A phase, B phase, and C phase, respectively. When at least two of them satisfy formula (8), it is determined that the current signal is inrush current, and then the differential protection device should be blocked. The algorithm flow of identifying the inrush current is shown in Figure 10.

6. Analysis of Simulation Results

The results of box dimension about fault currents are shown in Tables 1 and 2.

From Tables 1 and 2, it can be seen that at least two phase currents' box dimensions do not satisfy formula (8), so the signal is inner fault current.

Since the inrush current will be affected by various factors, the parameters of the simulation model are changed to obtain inrush current and box dimension D in different cases. Three-phase box dimension value D, when the transformer

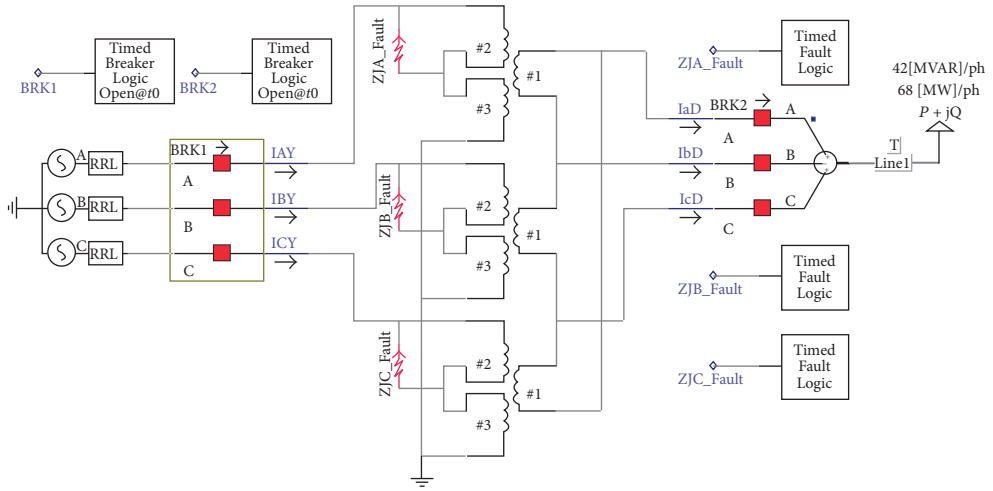

Figure 8: Simulation model of three-phase transformer inner fault.

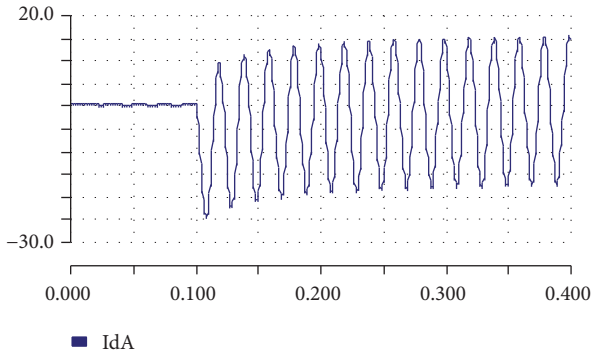

Figure 9: Waveform of turn-to-turn fault current.

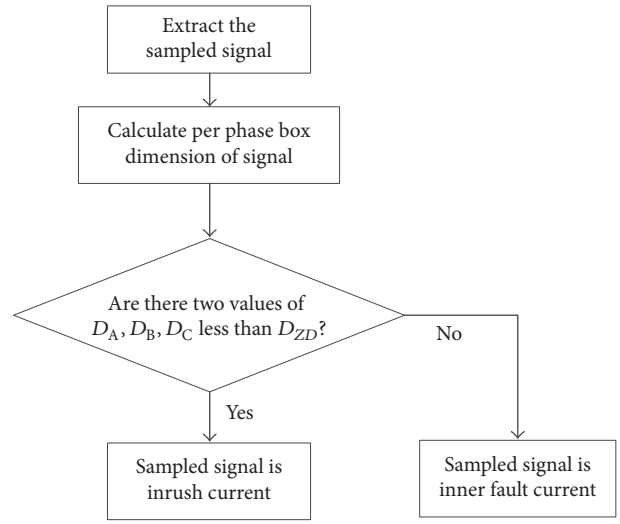

Figure 10: The flow of inrush current identification.

Table 3: Box dimensions of inrush current (remanence is 0).

No-load closing angle	D_A	D_B	D_C
0°	1.3565	1.3026	1.3559
30°	1.3772	1.3464	1.3712
60°	1.3011	1.3563	1.3561
90°	1.3714	1.3740	1.3766
120°	1.3558	1.3564	1.3017
150°	1.3172	1.3771	1.3464
180°	1.3561	1.3039	1.3562

Table 4: Box dimensions of inrush current (closing angle is 0°).

Remanence (T)	D_A	D_B	D_C
0.2	1.3224	1.3060	1.3229
0.4	1.3523	1.2938	1.3528
0.6	1.3418	1.3128	1.3447
0.8	1.3691	1.3351	1.3722

remanence is 0 and the closing phase varies, is shown in Table 3.

Three-phase box dimensions D, when the no-load closing angle is set to 0° and the transformer remanence varies, are shown in Table 4.

From Tables 3 and 4, it can be seen that the box dimensions D_A, D_B, and D_C satisfy formula (8). Therefore, the criterion can accurately identify the inrush current. The differential protection device can be blocked correctly.

7. Conclusion

In this paper, after establishing the simulation model, the difference between the waveform of the inrush current and the fault current is analyzed. The proposed algorithm is used to calculate the box dimension of the different signals. Then the box dimension is compared with the setting value D_{ZD}. The algorithm has been tested by MATLAB; the results show that the algorithm is simple to implement and calculate and also has high accuracy.

Conflicts of Interest

The authors declare that there are no conflicts of interest regarding the publication of this paper.

Acknowledgments

The authors acknowledge the financial support from Shandong Provincial Natural Science Foundation, China (ZR2016EEP10), Scientific Research Foundation of Shandong University of Science and Technology for Recruited Talents (2015RCJJ073), and Shandong Provincial Planning and Project, China (J17KA074).

References

[1] W. Chandrasena, P. G. McLaren, U. D. Annakkage, and R. P. Jayasinghe, "An improved low-frequency transformer model for use in GIC studies," *IEEE Transactions on Power Delivery*, vol. 19, no. 2, pp. 643–651, 2004.

[2] L. Zhang, P. Lv, H. Shen et al., "Analysis on protective relaying and its operation conditions of SGCC in 220 kV and above voltage AC systems in 2013," *Power System Technology*, vol. 39, no. 4, pp. 1153–1159, 2015.

[3] G. Maofa, H. Linyuan, and S. Danmiao, "Research of inrush current identification based on wavelet and modulus maximum," *Electrical Measurement & Instrument*, vol. 53, no. 17, pp. 29–33, 2016.

[4] G. Maofa, X. Wenhua, and L. Guoliang, "Identification of transformer inrush current based on hilbert spectrum," *Electrical Measurement & Instrument*, vol. 49, no. 556, pp. 47–50, 2012.

[5] J. Ma, Z. Wang, and Z. Wang, "Identify inrush current based on frequency characteristics of grille curve," *Electric Power Automation Equipment*, vol. 28, no. 7, pp. 29–36, 2008.

[6] G. Maofa, L. Meirong, and Y. Fanjiao, "Identification of transformer inrush current based on hilbert spectrum," *Electrical Measurement & Instrument*, vol. 52, no. 6, pp. 124–128, 2015.

[7] H. Jiadong and L. Weiqiang, "New algorithm to identify inrush current based on improved mathematical morphology," *Proceedings of the CSEE*, vol. 29, no. 7, pp. 98–105, 2009.

[8] X. Quanmin, L. Yuan, and Z. Minshou, "Blasting vibration signal analysis with wavelet and fractal portfolio analysis technique," *Journal of Vibration and Shock*, vol. 30, no. 12, pp. 120–124, 2011.

[9] A. Jayaprakash, G. R. Reddy, and N. Prasad, "Small target detection within sea clutter based on fractal analysis," *Procedia Technology*, vol. 24, pp. 988–995, 2016.

[10] Y. Qun and C. Na, *Modeling and Simulation of MATLAB/Simulink Power System*, China Machine Press, Beijing, China, 2013.

[11] M. Bouda, J. S. Caplan, and J. E. Saiers, "Box-counting dimension revisited: presenting an efficient method of minimizing quantization error and an assessment of the self-similarity of structural root systems," *Frontiers in Plant Science*, vol. 7, no. 402, article 149, 2016.

[12] X. Qi, X. Yin, and Z. Zhang, "Sympathetic inrush current in a transformer and a method for its identification," *IEEJ Transactions on Electrical and Electronic Engineering*, vol. 11, no. 4, pp. 442–450, 2016.

[13] Q. H. Wu, J. F. Zhang, and D. J. Zhang, "Ultra-high-speed directional protection of transmission lines using mathematical morphology," *IEEE Transactions on Power Delivery*, vol. 18, no. 4, pp. 1127–1133, 2003.

[14] S. T. Kim, B. G. Jin, S. J. Lee et al., "v-i trend-based protective relaying algorithm for 3-phase power transformer," in *Proceedings of the Power Engineering Society Summer Meeting*, pp. 605–610, IEEE, 2001.

[15] Y.-C. Kang, S.-H. Ok, and S.-H. Kang, "A CT saturation detection algorithm," *IEEE Transactions on Power Delivery*, vol. 19, no. 1, pp. 78–85, 2004.